Traffic 2011; **12:** 754–761

doi:10.1111/j.1600-0854.2011.01183.x

Clathrin Heavy Chain Gene Fusions Expressed in Human Cancers: Analysis of Cellular Functions

Maria K. E. Blixt and Stephen J. Royle*

Physiological Laboratory and Cancer Research UK Centre, University of Liverpool, Crown Street, Liverpool, L69 3BX, UK
**Corresponding author: Stephen J. Royle, s.j.royle@liverpool.ac.uk*

Clathrin is a protein expressed ubiquitously that has important functions in membrane trafficking and mitosis. Two different gene fusions involving clathrin heavy chain (CHC) have been described in human cancers. These involve either anaplastic lymphoma kinase (ALK) or transcription factor binding to IGHM enhancer 3 (TFE3) and raise the possibility that altered clathrin function in cells expressing the fusion proteins could contribute to oncogenesis. In the present study, we tested the functions of CHC-ALK and CHC-TFE3 in endocytosis and mitosis. CHC-ALK is comparable to full-length CHC in both functions indicating that malignant transformation in cells expressing CHC-ALK is not because of any change in clathrin function. CHC-TFE3 is not functional in endocytosis, but can substitute for CHC in mitosis. CHC-TFE3 causes prolonged interphase that is attributed to the TFE3 portion of the protein. We also describe how CHC-TFE3 is a dimer. This suggests that clathrin's proposed role in intermicrotubule bridging can be fulfilled not only by trimers but also by dimers. Finally, this study shows that the membrane trafficking and mitotic functions of clathrin are independent and separable.

Key words: ALK, cancer, cell cycle, clathrin, endocytosis, microtubule, mitosis, TFE3

Received 11 November 2010, revised and accepted for publication 28 February 2011, uncorrected manuscript published online 1 March 2011, published online 24 March 2011

Clathrin is a trimeric assembly, or triskelion, consisting of three heavy (~190 kDa) chains, each with an associated light (25–27 kDa) chain (1–3). Two clathrin heavy chain (CHC) genes exist in humans: *CHC17* (*CLTC* at 17q11-qter) and *CHC22* (*CLTCL1* at 22q11.21) (4,5). *CHC17*, referred to herein as CHC, is expressed constitutively at high levels in all cells, whereas the expression of *CHC22* is very low in most cells but is upregulated in skeletal muscle. In non-dividing cells, clathrin forms coats on membranes destined for vesicular transport either from the plasma membrane to endosomes or between endosomes and the *trans* Golgi network (6). When the cell enters mitosis, membrane trafficking is inhibited (7,8) and a subset of clathrin becomes localized to the mitotic spindle (9–11). The function of clathrin here is to stabilize the kinetochore fibers (K-fibers) of the mitotic spindle. It is proposed that clathrin achieves this by acting as an intermicrotubule bridge (5,11–15). Whether CHC22 is functionally different from CHC17 is currently debated (12,16,17), but its expression is too low in most cells to account for any redundancy of function following the depletion of CHC17 (12,16) and it will not be considered further here.

CHC is involved in two different types of gene fusion in human cancers. Anaplastic lymphoma kinase (ALK)-positive non-Hodgkin's lymphomas frequently contain a fusion protein involving clathrin: CHC-ALK. CHC-ALK has been reported in anaplastic null/T-cell lymphoma (18,19), ALK+ diffuse large B-cell lymphoma (20–27) and a rare non-lymphoid neoplasm, inflammatory myofibroblastic tumor (28,29). Furthermore, a fusion of *CLTC* with the C-terminal region of transcription factor binding to IGHM enhancer 3 (CHC-TFE3) has been reported in one case of pediatric renal cell carcinoma (30). A schematic diagram in Figure 1A shows the secondary structures of CHC (1675 residues), ALK (1620 residues) and TFE3 (575 residues). CHC-ALK is formed by chromosomal translocation t(2;17)(p23;q23) and results in the fusion of CHC (aa 1-1634) to the C-terminus of ALK (aa 1058-1620). This breakpoint is similar to other ALK fusions, e.g. nucleophosmin-ALK (NPM-ALK) at t(2;5)(p23;q35) (31). For CHC-TFE3, CHC (aa 1-932) is fused to the C-terminus of TFE3 (aa 295-575) by chromosomal translocation t(X;17)(p11.2;q23). CHC-ALK is predicted to be a trimer due to the preservation of the trimerization domain of CHC. In CHC-TFE3, the fusion excludes the trimerization domain of CHC, but includes the helix-loop-helix leucine zipper (HLH-LZ) of TFE3 that may mediate dimerization. It is unknown whether or not either of these proteins are functional.

Expression of other ALK-fusion proteins, e.g. NPM-ALK, is sufficient to cause cancer (33). Stat3 activation is required for ALK-mediated lymphomagenesis (33). However, it was reported that CHC-ALK does not activate Stat3 (34), which raised the possibility that perturbed clathrin function may play a role in oncogenesis, although a later study concluded that CHC-ALK may activate Stat3 (35). The oncogenic mechanism following the expression of CHC-TFE3 is also unclear. Although differences in the function of various ALK-fusion proteins suggest a contribution from the N-terminal partner, e.g. ability to multimerize, subcellular distribution, rates of proliferation and differential activation of signaling pathways (34), the specific contribution of N-terminal portions of these fusion proteins has so far been overlooked (36). Since the discovery of a role for clathrin in cell division, we set out to determine what effect the gene fusions have on clathrin function. This would allow us to assess what contribution clathrin has in malignant transformation of cells expressing clathrin gene fusions.

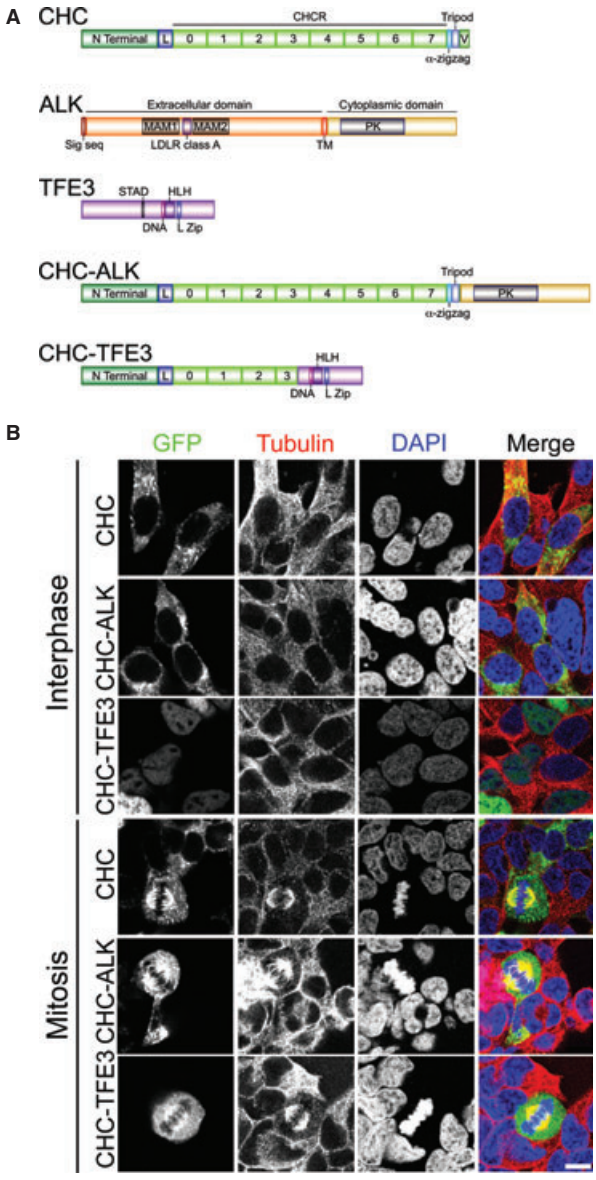

Figure 1: Clathrin heavy chain-gene fusion proteins. A) Schematic diagram to illustrate the secondary structures of predicted CHC-fusion proteins. CHC (aa 1-1675) comprises an N-terminal domain, linker region (L), CHCR 0–7, α-zigzag and a trimerization domain followed by a variable region (V) (32). ALK (aa 1-1620) is a receptor tyrosine kinase, with extracellular, transmembrane (TM) and cytoplasmic domains. The extracellular domain has two meprin/A5/mu (MAM) domains and an intervening LDLR class A repeat. TFE3 (aa 1-575) is a transcription factor with a strong transactivation domain (STAD), DNA-binding basic motif (DNA), basic helix-loop-helix (bHLH) and leucine zipper (L Zip) domains. CHC-ALK comprises CHC (aa 1-1634) fused to the C-terminus of ALK (aa 1058-1620), whereas CHC-TFE3 comprises CHC (aa 1-932) fused to the C-terminus of TFE3 (aa 295-575). B) Representative confocal images to show the subcellular distributions of GFP-CHC, GFP-CHC-ALK and GFP-CHC-TFE3 expressed in HEK293 cells depleted of endogenous CHC. Cells in interphase (above) and mitosis (below) were fixed and co-stained for tubulin. Scale bar, 10 μm.

Results and Discussion

The subcellular distributions of CHC-ALK and CHC-TFE3 were compared with that of CHC by expression of green fluorescent protein (GFP)-tagged versions of each protein in cells depleted of endogenous CHC. We found that GFP-CHC-ALK had a subcellular distribution that was very similar to GFP-CHC. GFP-CHC-ALK was found in numerous puncta, presumably pits and vesicles in the cytoplasm, and accumulated in a perinuclear region (Figure 1B). During mitosis, GFP-CHC-ALK, like GFP-CHC, was localized to the mitotic spindle (Figure 1B). GFP-CHC-TFE3, on the other hand, was localized exclusively to the nucleus in cells in interphase (Figure 1B). During mitosis, GFP-CHC-TFE3 was accumulated at the mitotic spindle in most cells. In cells with strong expression, GFP-CHC-TFE3 was accumulated at puncta on mitotic chromosomes. These puncta were not centromeres/kinetochores as they were too few in number and they did not colocalize with anti-CENP-B or CREST and may represent protein aggregates. The subcellular localizations of GFP-CHC-ALK and GFP-CHC-TFE3 were similar to that previously reported in clinical samples expressing CHC-ALK and CHC-TFE3 processed for immunohistochemistry (18,30).

To assess the cellular functions of CHC-ALK and CHC-TFE3, we examined the ability of each protein to 'rescue' those functions that are affected by the depletion of CHC. In each assay, the following conditions were compared: 'Control' (GFP coexpressed with control shRNA), 'GFP' (GFP coexpressed with CHC shRNA) and 'CHC', 'CHC-ALK', 'CHC-TFE3' (GFP-tagged CHC gene fusions coexpressed with CHC shRNA).

The endocytic function of clathrin gene fusion proteins was tested by assaying their ability to uptake fluorescent transferrin. As previously described, the uptake of transferrin (50 μg/mL for 10 min) was inhibited by clathrin depletion and the uptake was rescued by the expression of GFP-CHC (13). GFP-CHC-ALK, but not GFP-CHC-TFE3, was able to rescue normal endocytosis (Figure 2). This suggests that the fusion of ALK at the C-terminus of CHC does not inhibit trimerization nor does it interfere with any regions of CHC needed for interactions with other CHCs for lattice formation. CHC-TFE3, on the other hand, could not uptake transferrin (Figure 2). This result is perhaps not surprising as the gene fusion interferes with trimerization and removes many of the clathrin heavy chain repeat (CHCR) regions needed for lattice formation (Figure 1A). Moreover, during interphase, CHC-TFE3 is localized to the nucleus and is therefore not in the correct location for endocytosis (Figure 2).

We next tested for the rescue of normal mitosis by CHC-ALK and CHC-TFE3 in clathrin-depleted cells. Quantification of the mitotic index in asynchronous transfected cells showed that clathrin depletion resulted in a three-fold increase, indicating a longer time spent in mitosis. This change was rescued by GFP-CHC, GFP-CHC-ALK

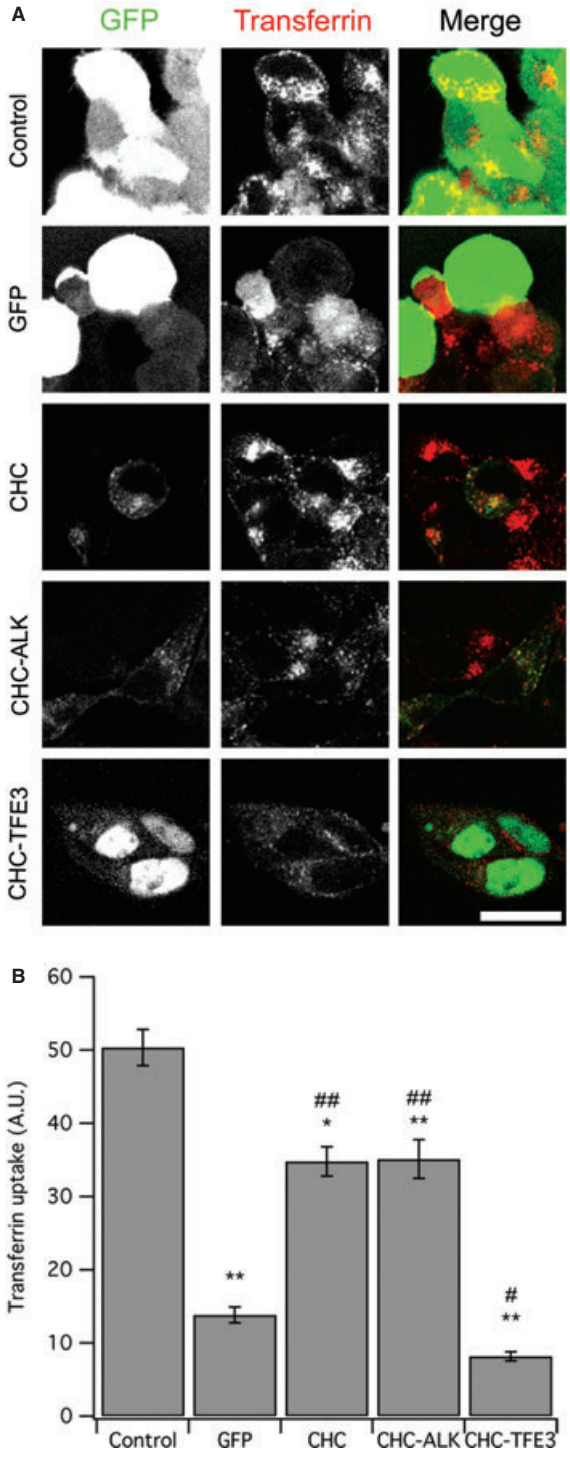

Figure 2: Assessment of endocytic function of CHC-fusion proteins. A) Representative confocal micrographs to show transferrin uptake. Scale bar, 20 μm. B) Bar chart of quantification of transferrin uptake. Control is GFP expressed on a control RNAi background. The remainder expresses the indicated GFP-tagged construct on a CHC RNAi background. Results are mean ± SEM of 93–106 cells per condition, $n_{exp} = 3$, * or $^{\#}p < 0.05$, ** or $^{\#\#}p < 0.01$. Asterisks and hashes indicate difference from control and GFP, respectively.

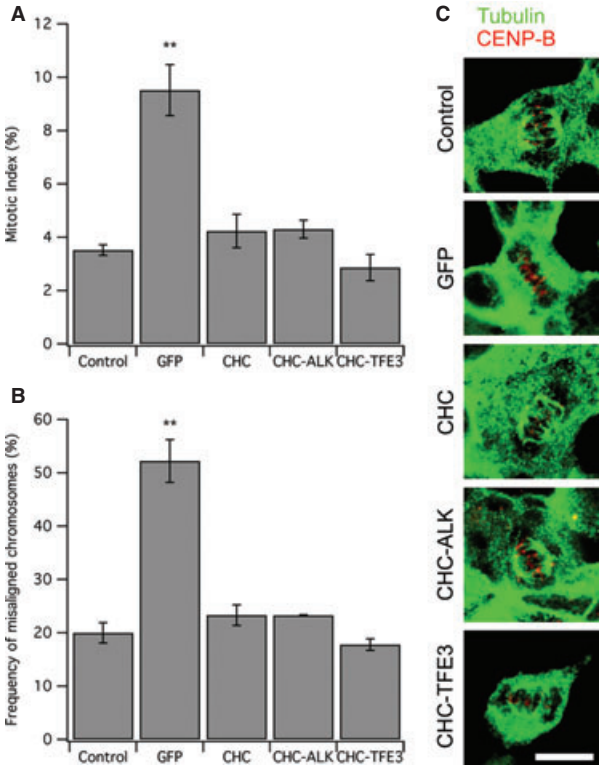

Figure 3: Assessment of mitotic function of CHC-fusion proteins. A) Bar chart to show the mean mitotic index ± SEM, $n_{exp} = 5$, $^{**}p < 0.01$. B) Bar chart to show the mean frequency of misaligned chromosomes in metaphase-like cells, ± SEM, $n_{exp} = 3$, $^{**}p < 0.01$. C) Representative fluorescence micrographs to show cold-stable K-fiber attachments. Cells were fixed and stained with anti-tubulin (green) and anti-CENP-B (red). Fluorescence confirmed that cells were expressing the indicated construct (not shown). Scale bar, 10 μm.

and GFP-CHC-TFE3 (Figure 3A). We also quantified the frequency of transfected metaphase-like cells with misaligned chromosomes. These data were correlated with the mitotic index measurements, with control cells showing ∼20%, rising to ∼50% upon clathrin depletion and a rescue with GFP-CHC, GFP-CHC-ALK and GFP-CHC-TFE3 (Figure 3B). A final qualitative assay of clathrin function in mitosis was carried out: the ability to stabilize K-fibers. In this assay, cells at metaphase are briefly chilled to depolymerize any non-stable K-fibers. GFP cells, but not controls, showed missing K-fibers following this manipulation (Figure 3C). K-fibers were cold-stable in CHC, CHC-ALK or CHC-TFE3 cells. This result, although qualitative only, agrees with the measurements of rescue of mitotic index and the frequency of misaligned chromosomes. Interestingly, the expression of GFP-CHC-TFE3 appeared to be a more effective rescue protein compared with GFP-CHC (mitotic index of CHC versus CHC-TFE3, $p = 0.0213$). The reduction in mitotic index relative to 'GFP' could be because of rescue of mitosis and/or other changes in the cell cycle. Although the rescue of chromosome alignment and of K-fiber stability indicates

that the reduction in mitotic index is not solely because of other changes in the cell cycle.

This difference prompted us to examine how cells progressed through mitosis. To do this, we arrested cells at the G2/M boundary using 30 ng/mL nocodazole and monitored the mitotic profiles of the cells at 0, 45 and 90 min following their release. Immediately after release, the majority of mitotic cells are arrested in prometaphase (Figure 4A). With the exception of GFP, all conditions passed through mitosis similarly, indicating that GFP-CHC, GFP-CHC-ALK and GFP-CHC-TFE3 gave a functional rescue of mitosis. This suggests that the reduction in mitotic index to below control levels seen previously with GFP-CHC-TFE3 is likely to be due in part but not wholly to changes in cell cycle timings outside M-phase.

It was noted that the number of cells arrested by the nocodazole treatment was lower in GFP-CHC-TFE3 than in any of the other conditions (Figure 4A). To investigate this further, we tested what proportion of cells we arrest at the G2/M boundary with a 16-h nocodazole treatment. Figure 4B shows that in 16 h we arrested ~60% of control or GFP cells, whereas only half of this fraction was arrested in GFP-CHC-TFE3 cells. To test whether this was related to CHC depletion and rescue or to expression of GFP-CHC-TFE3 itself, the fusion protein was expressed on a normal background. This resulted in a similar low capture of cells at G2/M by nocodazole. The nocodazole blockade is sound as virtually all the cells that are arrested in mitosis were blocked at prometaphase, whereas this would be lower if cells were slipping through the nocodazole block. This result indicates that there is a delay in non-M-phase

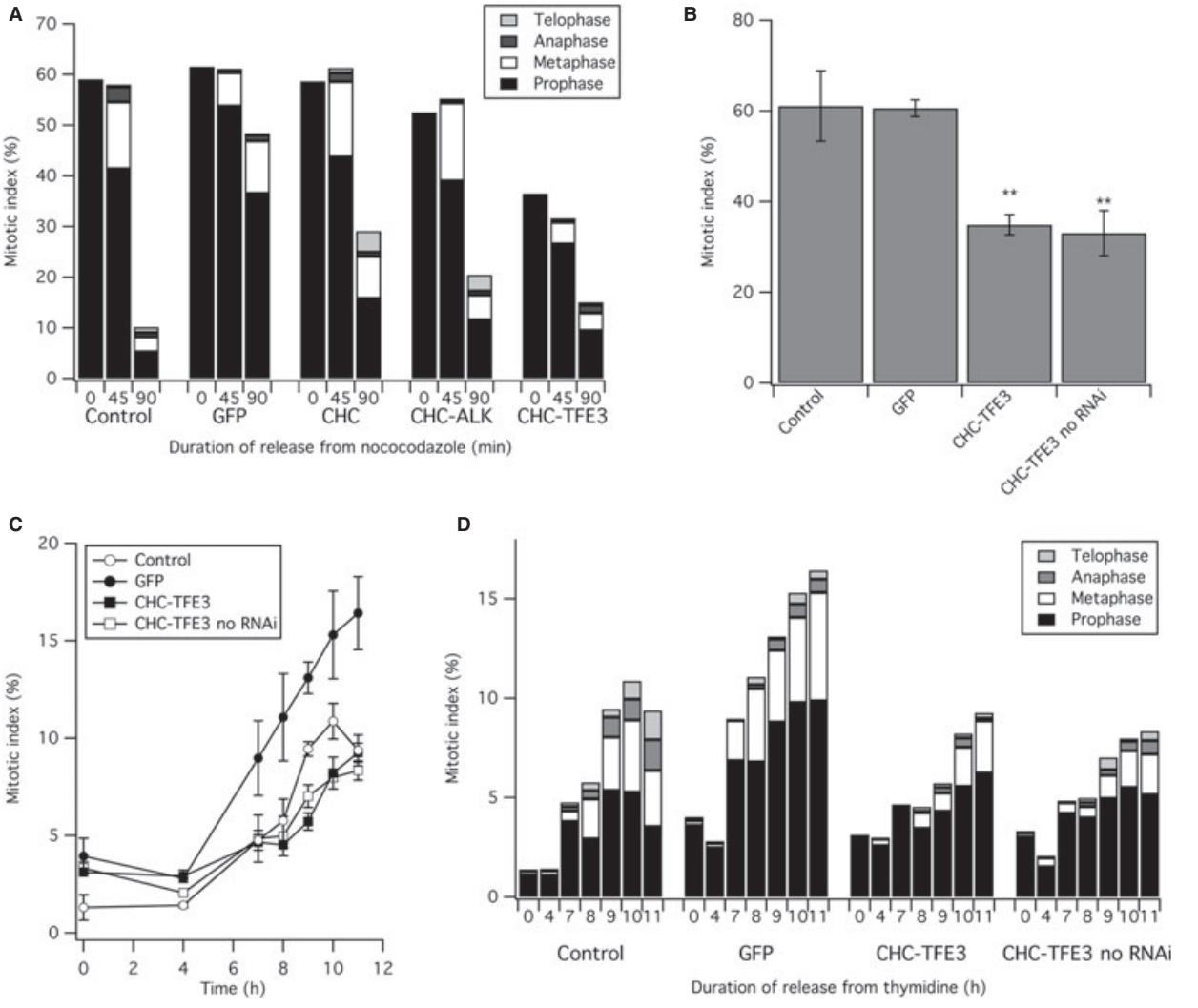

Figure 4: Effect of CHC-TFE3 on cell cycle progression. A) Bar chart to show the progression of the cells through mitosis after release from nocodazole treatment. The mean percentage of transfected cells at each stage of mitosis is indicated. B) Bar chart to show the mean ± SEM. Mitotic index of cells treated for 16 h with nocodazole (40 ng/mL). **$p < 0.01$. C) A plot of mitotic index as a function of duration of release from thymidine blockade. Markers indicate mean ± SEM. D) Bar chart to show the mean percentage of cells at each stage of mitosis after various durations of release from thymidine blockade.

regions of the cell cycle in cells expressing GFP-CHC-TFE3 and that this is unrelated to CHC depletion.

To test this hypothesis, we next examined how cells expressing GFP-CHC-TFE3 progress through the cell cycle when released from blockade at the G1/S boundary. Cells were arrested at G1/S with a double-thymidine block protocol and were analyzed at various times after release (Figure 4C). Control and GFP cells began to enter mitosis at around 7 h after release. GFP cells accumulated in mitosis, a result of the delay at prometaphase upon clathrin depletion (11). The greater variability of the mean mitotic index in GFP cells likely reflects the variability of clathrin depletion across different experiments. GFP-CHC-TFE3 cells were delayed by approximately 2 h and this delay was unaffected by the depletion of endogenous CHC. Again, the progression through mitosis appeared normal for cells expressing GFP-CHC-TFE3 (Figure 4D). Together, these results confirmed that cells expressing GFP-CHC-TFE3, regardless of endogenous clathrin levels, are delayed in interphase. As this was independent of CHC, it indicates that CHC-TFE3 has a dominant effect on prolonging interphase probably by alteration of the expression of genes that are regulated by TFE3. The delay in S/G2 observed after release from double-thymidine block (Figure 4C) could only partially account for the difference observed in nocodazole arrest (Figure 4B). In those experiments, nocodozole treatment of asynchronous cells for 16 h arrested approximately half the number of cells expressing GFP-CHC-TFE3 compared to the controls. Mitotic exit is apparently normal (Figure 4A), which suggests that interphase is approximately twice as long. Lengthening S/G2 by 2 h (~125% of controls) cannot by itself account for this difference. We therefore predict that in G1 a similar or longer delay occurs.

How can CHC-TFE3 rescue mitosis in cells depleted of CHC? It is thought that clathrin's mitotic function of stabilizing K-fibers is by clathrin acting as an intermicrotubule bridge (11,13,15). We have previously shown that trimerization of clathrin is critical for its mitotic function (13). The trimerization domain of CHC is preserved in CHC-ALK, whereas it is absent in CHC-TFE3 (Figure 1A). We tested whether the basic helix-loop-helix and leucine zipper motifs present in CHC-TFE3 could mediate alternative multimerization, i.e. dimerization. To do this, CHC or CHC-TFE3 was tagged at the N-terminus with either Myc or Flag epitope tags. These constructs were then expressed singly or pairwise in human embryonic kidney (HEK293) cells (Figure 5A). Immunoprecipitation (IP) of Flag-CHC or Flag-CHC-TFE3 resulted in the coprecipitation of Myc-CHC or Myc-CHC-TFE3, respectively. Mixing the singly transfected cell lysates prior to IP did not result in co-IP, which indicated that the interaction was the result of specific assembly of Flag- and Myc-tagged multimers in cells.

The bHLH-LZ motifs in TFE3 are thought to mediate homodimerization of this transcription factor. As our co-IP experiments suggested that CHC-TFE3 exists as a

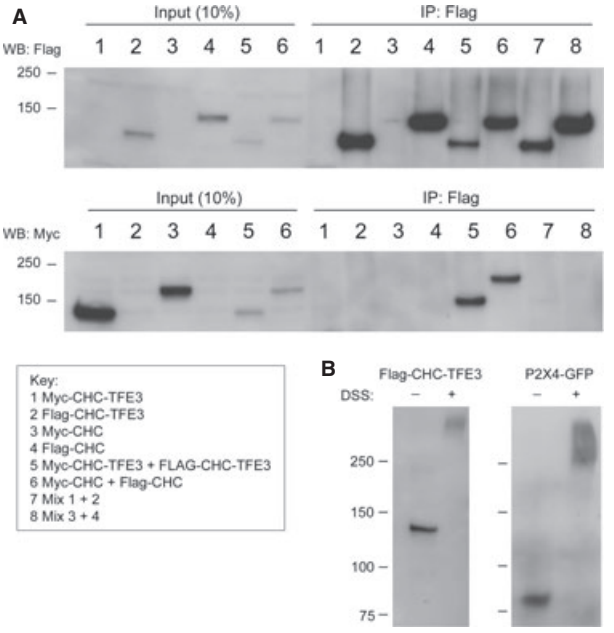

Figure 5: CHC-TFE3 is a dimer. A) Whole-cell lysates from HEK293 cells transfected as indicated were lysed and immunoprecipitated with anti-Flag and samples from inputs (10%) and IPs were analyzed by western blotting with anti-Flag or anti-Myc. Lanes 7 and 8 show no bands for anti-Myc, confirming that multimerization of proteins does not occur *in vitro*. Note that in the IP samples, bands have a slightly lower mobility. B) Lysates from HEK293 cells expressing either Flag-CHC-TFE3 or P2X4-GFP were cross-linked with DSS, separated by SDS–PAGE and subsequently western blotted with anti-Flag or anti-GFP, respectively. Approximate molecular weights (kDa) are as indicated to the left.

multimer, we next tested whether CHC-TFE3 was a dimer by cross-linking Flag-CHC-TFE3 using disuccinimidyl suberate (DSS) and analyzing the protein using SDS–PAGE and western blotting using anti-FLAG. As a positive control for cross-linking, we used P2X4-GFP, a known homotrimer (37,38). Upon DSS treatment, the band for FLAG-CHC-TFE3 shifted from ~140 to ~300 kDa, consistent with homodimer formation (Figure 5B). The band for P2X4-GFP showed a shift from ~80 to ~260 kDa, which was consistent with homotrimer formation. This suggests that the dimerization motifs in TFE3 are functional in CHC-TFE3 and that CHC-TFE3 exists as a dimer. As CHC-TFE3 was able to rescue the mitotic defects caused by clathrin depletion, the implication here is that dimerized clathrin may be just as efficient as trimeric clathrin in terms of its mitotic function.

In this study, we have shown that CHC-ALK is fully functional in our assays of endocytic and mitotic functions. Any contribution of CHC-ALK to malignant transformation of cells expressing this fusion is not because of perturbation of clathrin function. It seems likely therefore that the strong constitutive expression of CHC results in robust expression of CHC-ALK and that the tyrosine

kinase activity of ALK is transactivated due to the obligatory trimerization of CHC-ALK. By contrast, CHC-TFE3 was non-functional in endocytosis but could operate in mitosis. We have previously identified a truncation mutant of CHC that is functional in endocytosis but not mitosis (12). The present work with CHC-TFE3 leaves little doubt that the functions of clathrin in endocytosis and mitosis are distinct and separable. Several proteins with roles in membrane trafficking during interphase have mitotic 'moonlighting' functions (39,40). This has led to the proposal that membrane trafficking and mitosis are intrinsically linked (39) or that mitotic spindle function can be modulated by a membranous matrix that in turn is regulated by trafficking (40). There may indeed be linkage or cross-talk between these two important cellular functions, but our present findings argue that, at least for clathrin, there is no evidence for this. Finally, if the 'bridge hypothesis' for clathrin function in mitosis is correct, then the prospect of dimeric CHC-TFE3 bridges rather than trimeric inter-microtubule cross-links is an unexpected and intriguing notion that will be explored further.

Materials and Methods

Molecular biology

The pBrain strategy to knockdown endogenous CHC17 by RNAi and to re-express GFP-tagged proteins was employed as described previously (11–13). The plasmids pBrain-GFP-CHC1 (control), pBrain-GFP-CHC4 (GFP), pBrain-GFP-CHC(1-1675)-KDP-CHC4 (CHC17) and GFP-P2X4 were available from previous work (11,13,41).

ALK cDNA (RMS17-2) was a kind gift of Stephan Morris (St. Jude Children's Research Hospital). CHC-ALK was made by overlap extension polymerase chain reaction (PCR) and inserted into *Xba*I-*Mlu*I of pDiddy-GFP-CHC(1-1639)KDP-CHC4. A *Mlu*I-*Mlu*I fragment from pEGFP-C1 was ligated at *Mlu*I to repair the polyA sequence in the vector and give pDiddy-GFP-CHC-ALKKDP-CHC4. The pDiddy and pBrain systems are interchangeable (13).

TFE3 cDNA was purchased from Geneservice (TFE3, mRNA MGC: 39177, IMAGE: 4576858). GFP-CHC-TFE3 was made by taking advantage of an *Ase*I site next to the fusion site (after aa 932). A PCR fragment comprising TFE3 residues 296-575 was ligated into GFP-CHC(1-1675)KDP at *Ase*I(partial)-*Xma*I. This was converted to pBrain-GFP-CHC-TFE3KDP-CHC4 by ligation of an *Apa*LI-*Apa*LI fragment from pBrain-GFP-CHC(1-1675)KDP-CHC4.

To make Flag- and Myc-tagged constructs, oligonucleotides were annealed and inserted in place of GFP at *Age*I-*Bgl*II in pEGFP-C1. All constructs were verified by restriction digest and automated DNA sequencing (GATC).

Cell biology

HEK293 cells were cultured in DMEM containing 10% fetal bovine serum and 100 U/mL penicillin–streptomycin at 37°C and 5% CO_2. Cells were plated onto poly-L-lysine-coated coverslips at a density of 40 000–70 000/mL. Transfection was carried out the next day using the calcium phosphate method. Briefly, 1 h before transfection the medium is replaced with 1 mL of fresh medium. For one well of a six-well plate (two coverslips), 5 μL of 2.5 M $CaCl_2$ and 1.25 μg of DNA were mixed with 0.1× TE buffer [1 mM Tris–Cl, 0.1 mM ethylenediaminetetraacetic acid (EDTA), pH 7.6] to make up to 50 μL. A 50 μL of 2× HEPES buffer (140 mM NaCl, 1.5 mM Na_2HPO_4, 50 mM HEPES, pH 7.05) was added and left for 1 min at 37°C to allow precipitate to form. Precipitate was added to the cells and the media changed 6 h later.

All cells were analyzed 3 days post-transfection, when knockdown was maximal (11). For measurements of mitotic index, misaligned chromosomes, transferrin uptake, K-fiber stability, cells were fixed in 3% paraformaldehyde/4% sucrose in PBS for 10 min and coverslips were mounted using Mowiol 4-88, 4′,6-diamidino-2-phenylindole 10 μg/mL.

For immunocytochemistry, cells were fixed as described above, permeabilized for 10 min in PBS containing 0.5% Triton-X-100 and blocked for 2 h in blocking solution (3% BSA, 5% goat serum in 1× PBS). The primary and secondary antibodies were made up in blocking solution and left on for 2 and 1 h, respectively, the cells were washed 3× for 5 min in PBS after the primary and secondary antibody incubations. The coverslips were then mounted as above.

For qualitative assessment of K-fiber stability, growth medium was exchanged for ice-cold DMEM and the cells were put on ice for 5 min. Cells were then fixed, stained and mounted.

For transferrin uptake, cells were serum starved in DMEM for 30 min, transferrin-Alexa-Fluor 546 (Invitrogen) was added (1:100 in DMEM, 5 mg/mL stock) for 10 min, all at 37°C and 5% CO_2, then fixed and mounted.

For nocodazole treatment, at 53–55 h post-transfection nocodazole (30 ng/mL) was added. After 16 h, cells were washed 3× in warm DMEM and then growth medium was added. After 0, 45 or 90 min, the cells were washed in PBS, fixed and mounted.

For thymidine treatment, at 20–30 h post-transfection thymidine (2 mM) was added. After 16 h, the cells were washed 3× in warm DMEM and then growth medium was added. After 7 h, thymidine (2 mM) was added and incubated for 16 h. Cells were then washed as before and fixed after various time-points of release.

Antibodies

Antibodies used were monoclonal anti-Flag (Sigma-Aldrich), monoclonal anti-cMyc (9E10, purified in-house) and polyclonal anti-GFP (generous gift from Francis Barr, University of Liverpool, UK). For immunoblotting, antibody concentrations were as follows: 1:500 anti-Flag, 1:200 anti-cMyc and 1:1000 anti-GFP. Anti-mouse horseradish peroxidase (HRP)-conjugated immunoglobulin G (IgG) (GE Healthcare; 1:10 000) and anti-sheep HRP-conjugated IgG (Cambridge Bioscience; 1:10 000) were used for detection. For immunofluorescence, primary antibodies used were rabbit-anti-β-tubulin (Abcam) and mouse-anti-CENP-B (generous gift from Bill Earnshaw, University of Edinburgh, UK). Secondary antibodies used were goat-anti-rabbit Alexa 568 and goat-anti-mouse Alexa 633 (Invitrogen). Antibody concentrations were as follows: 1:1000 anti-β-tubulin, 1:1000 anti-CENP-B and 1:500 Alexa 568/633.

Biochemistry

For whole-cell lysates, cells were lysed in buffer A (20 mM Tris, pH 7.5, 150 mM NaCl, 1% Igepal, 15 μg/mL DNAse, 30 mM NaF, 5 mM Na_3Vo_4, 100 nM okadaic acid, protease inhibitor cocktail). Samples were incubated on ice for 30 min and lysates were cleared by centrifugation at 20 800 × *g* for 2 × 15 min at 4°C. The supernatant was retained as cell lysate.

For IPs, 200 μg of lysate was precleared with 15 μL of protein G beads for 1.5 h at 4°C, rotating, then incubated with 2.5 μg of Flag antibody for 1 h at 4°C, rotating. Ten microliters of protein G beads was then added and incubated for a further 1 h at 4°C, rotating. Beads were washed once with 1 mL of buffer B (20 mM Tris, pH 7.5, 150 mM NaCl, 1% Igepal, protease inhibitor cocktail) and 4–6× with 0.5–1 mL of wash buffer (20 mM Tris, pH

7.5, 150 mM NaCl, 0.1% Igepal, protease inhibitor cocktail), resuspended in Laemmli buffer and analyzed by SDS–PAGE and immunoblotting.

For cross-linking experiments, the cross-linking reagent DSS (Pierce) was freshly prepared in DMSO, diluted to a final concentration of 0.5 mM and incubated with the lysate (15 μg CHC-TFE3 and 7.5 μg P2X4) at room temperature for 5 min. Control samples without cross-linker were incubated with DMSO only. The reaction was quenched by the addition of Tris–Cl, pH 7.5, to a final concentration of 50 mM and incubated for 30 min at room temperature. All samples were mixed with Laemmli buffer and analyzed by SDS–PAGE and immunoblotting.

Imaging, quantification and analysis

All imaging, quantification and analysis was performed as described previously (12,13). Experiments were performed three or more times, with the exception of nocodazole release which was performed twice in duplicate. For mitotic index measurements, between 1916 and 2173 cells per condition were counted. For the misaligned chromosome measurements, 90 cells were analyzed for each condition. Cold-stable K-fibers in HEK293 cells were analyzed with a Leica CellR imaging system. Stacks of 10 images were taken at a depth of 16 bit and the middle four or five images were projected into a single image using ImageJ. For mitotic counts after release, between 553–994 cells per condition were counted. The transferrin uptake data were not normally distributed and were compared by Kruskal–Wallis test followed by Dunn's multiple comparison test. Binomial data were compared by chi-squared approximation. Calculations were performed with Minitab 15.1 (Minitab) or Instat3 (GraphPad). Figures were assembled using Igor Pro (Wavemetrics) and Adobe Photoshop.

Acknowledgments

We are very grateful to Samantha Williams for help with the DSS cross-linking experiments. We thank the members of the Royle lab for useful discussion and those who donated reagents for use in this study. This work was supported by a Cancer Research UK Career Establishment Award (C25425/A8722) to S. J. R.

References

1. Pearse BM. Coated vesicles from pig brain: purification and biochemical characterization. J Mol Biol 1975;97:93–98.
2. Ungewickell E, Branton D. Assembly units of clathrin coats. Nature 1981;289:420–422.
3. Kirchhausen T, Harrison SC. Protein organization in clathrin trimers. Cell 1981;23:755–761.
4. Wakeham DE, Abi-Rached L, Towler MC, Wilbur JD, Parham P, Brodsky FM. Clathrin heavy and light chain isoforms originated by independent mechanisms of gene duplication during chordate evolution. Proc Natl Acad Sci U S A 2005;102:7209–7214.
5. Royle SJ. The cellular functions of clathrin. Cell Mol Life Sci 2006;63:1823–1832.
6. Kirchhausen T. Clathrin. Annu Rev Biochem 2000;69:699–727.
7. Warren G. Membrane partitioning during cell division. Annu Rev Biochem 1993;62:323–348.
8. Schweitzer JK, Burke EE, Goodson HV, D'Souza-Schorey C. Endocytosis resumes during late mitosis and is required for cytokinesis. J Biol Chem 2005;280:41628–41635.
9. Maro B, Johnson MH, Pickering SJ, Louvard D. Changes in the distribution of membranous organelles during mouse early development. J Embryol Exp Morphol 1985;90:287–309.
10. Okamoto CT, McKinney J, Jeng YY. Clathrin in mitotic spindles. Am J Physiol Cell Physiol 2000;279:C369–C374.
11. Royle SJ, Bright NA, Lagnado L. Clathrin is required for the function of the mitotic spindle. Nature 2005;434:1152–1157.
12. Hood FE, Royle SJ. Functional equivalence of the clathrin heavy chains CHC17 and CHC22 in endocytosis and mitosis. J Cell Sci 2009;122:2185–2190.
13. Royle SJ, Lagnado L. Trimerisation is important for the function of clathrin at the mitotic spindle. J Cell Sci 2006;119:4071–4078.
14. Yamauchi T, Ishidao T, Nomura T, Shinagawa T, Tanaka Y, Yonemura S, Ishii S. A B-Myb complex containing clathrin and filamin is required for mitotic spindle function. EMBO J 2008;27:1852–1862.
15. Booth DG, Hood FE, Prior IA, Royle SJ. A TACC3/ch-TOG/clathrin complex stabilises kinetochore fibres by inter-microtubule bridging. EMBO J 2011;30:906–919.
16. Esk C, Chen CY, Johannes L, Brodsky FM. The clathrin heavy chain isoform CHC22 functions in a novel endosomal sorting step. J Cell Biol 2010;188:131–144.
17. Vassilopoulos S, Esk C, Hoshino S, Funke BH, Chen CY, Plocik AM, Wright WE, Kucherlapati R, Brodsky FM. A role for the CHC22 clathrin heavy-chain isoform in human glucose metabolism. Science 2009;324:1192–1196.
18. Touriol C, Greenland C, Lamant L, Pulford K, Bernard F, Rousset T, Mason DY, Delsol G. Further demonstration of the diversity of chromosomal changes involving 2p23 in ALK-positive lymphoma: 2 cases expressing ALK kinase fused to CLTCL (clathrin chain polypeptide-like). Blood 2000;95:3204–3207.
19. Cools J, Wlodarska I, Somers R, Mentens N, Pedeutour F, Maes B, De Wolf-Peeters C, Pauwels P, Hagemeijer A, Marynen P. Identification of novel fusion partners of ALK, the anaplastic lymphoma kinase, in anaplastic large-cell lymphoma and inflammatory myofibroblastic tumor. Genes Chromosomes Cancer 2002;34:354–362.
20. Gascoyne RD, Lamant L, Martin-Subero JI, Lestou VS, Harris NL, Muller-Hermelink HK, Seymour JF, Campbell LJ, Horsman DE, Auvigne I, Espinos E, Siebert R, Delsol G. ALK-positive diffuse large B-cell lymphoma is associated with clathrin-ALK rearrangements: report of 6 cases. Blood 2003;102:2568–2573.
21. Chikatsu N, Kojima H, Suzukawa K, Shinagawa A, Nagasawa T, Ozawa H, Yamashita Y, Mori N. ALK+, CD30-, CD20- large B-cell lymphoma containing anaplastic lymphoma kinase (ALK) fused to clathrin heavy chain gene (CLTC). Mod Pathol 2003;16:828–832.
22. De Paepe P, Baens M, van Krieken H, Verhasselt B, Stul M, Simons A, Poppe B, Laureys G, Brons P, Vandenberghe P, Speleman F, Praet M, De Wolf-Peeters C, Marynen P, Wlodarska I. ALK activation by the CLTC-ALK fusion is a recurrent event in large B-cell lymphoma. Blood 2003;102:2638–2641.
23. Gesk S, Gascoyne RD, Schnitzer B, Bakshi N, Janssen D, Klapper W, Martin-Subero JI, Parwaresch R, Siebert R. ALK-positive diffuse large B-cell lymphoma with ALK-clathrin fusion belongs to the spectrum of pediatric lymphomas. Leukemia 2005;19:1839–1840.
24. Isimbaldi G, Bandiera L, d'Amore ES, Conter V, Milani M, Mussolin L, Rosolen A. ALK-positive plasmablastic B-cell lymphoma with the clathrin-ALK gene rearrangement. Pediatr Blood Cancer 2006;46:390–391.
25. Rudzki Z, Rucinska M, Jurczak W, Skotnicki AB, Maramorosz-Kurianowicz M, Mruk A, Pirog K, Utych G, Bodzioch P, Srebro-Stariczyk M, Wlodarska I, Stachura J. ALK-positive diffuse large B-cell lymphoma: two more cases and a brief literature review. Pol J Pathol 2005;56:37–45.
26. Bubala H, Maldyk J, Wlodarska I, Sonta-Jakimczyk D, Szczepanski T. ALK-positive diffuse large B-cell lymphoma. Pediatr Blood Cancer 2006;46:649–653.
27. McManus DT, Catherwood MA, Carey PD, Cuthbert RJ, Alexander HD. ALK-positive diffuse large B-cell lymphoma of the stomach associated with a clathrin-ALK rearrangement. Hum Pathol 2004;35:1285–1288.
28. Bridge JA, Kanamori M, Ma Z, Pickering D, Hill DA, Lydiatt W, Lui MY, Colleoni GW, Antonescu CR, Ladanyi M, Morris SW. Fusion of the ALK gene to the clathrin heavy chain gene, CLTC, in inflammatory myofibroblastic tumor. Am J Pathol 2001;159:411–415.
29. Yamamoto H, Kohashi K, Oda Y, Tamiya S, Takahashi Y, Kinoshita Y, Ishizawa S, Kubota M, Tsuneyoshi M. Absence of human herpesvirus-8 and Epstein-Barr virus in inflammatory myofibroblastic tumor with anaplastic large cell lymphoma kinase fusion gene. Pathol Int 2006;56:584–590.
30. Argani P, Lui MY, Couturier J, Bouvier R, Fournet JC, Ladanyi M. A novel CLTC-TFE3 gene fusion in pediatric renal adenocarcinoma with t(X;17)(p11.2;q23). Oncogene 2003;22:5374–5378.
31. Morris SW, Kirstein MN, Valentine MB, Dittmer KG, Shapiro DN, Saltman DL, Look AT. Fusion of a kinase gene, ALK, to a

nucleolar protein gene, NPM, in non-Hodgkin's lymphoma. Science 1994;263:1281–1284.
32. Fotin A, Cheng Y, Sliz P, Grigorieff N, Harrison SC, Kirchhausen T, Walz T. Molecular model for a complete clathrin lattice from electron cryomicroscopy. Nature 2004;432:573–579.
33. Chiarle R, Simmons WJ, Cai H, Dhall G, Zamo A, Raz R, Karras JG, Levy DE, Inghirami G. Stat3 is required for ALK-mediated lymphomagenesis and provides a possible therapeutic target. Nat Med 2005;11:623–629.
34. Armstrong F, Duplantier MM, Trempat P, Hieblot C, Lamant L, Espinos E, Racaud-Sultan C, Allouche M, Campo E, Delsol G, Touriol C. Differential effects of X-ALK fusion proteins on proliferation, transformation, and invasion properties of NIH3T3 cells. Oncogene 2004;23:6071–6082.
35. Momose S, Tamaru J, Kishi H, Mikata I, Mori M, Toyozumi Y, Itoyama S. Hyperactivated STAT3 in ALK-positive diffuse large B-cell lymphoma with clathrin-ALK fusion. Hum Pathol 2009;40:75–82.
36. Duyster J, Bai RY, Morris SW. Translocations involving anaplastic lymphoma kinase (ALK). Oncogene 2001;20:5623–5637.
37. Boumechache M, Masin M, Edwardson JM, Gorecki DC, Murrell-Lagnado R. Analysis of assembly and trafficking of native P2X4 and P2X7 receptor complexes in rodent immune cells. J Biol Chem 2009;284:13446–13454.
38. Barrera NP, Ormond SJ, Henderson RM, Murrell-Lagnado RD, Edwardson JM. Atomic force microscopy imaging demonstrates that P2X2 receptors are trimers but that P2X6 receptor subunits do not oligomerize. J Biol Chem 2005;280:10759–10765.
39. Scita G, Di Fiore PP. The endocytic matrix. Nature 2010;463: 464–473.
40. Zheng Y. A membranous spindle matrix orchestrates cell division. Nat Rev Mol Cell Biol 2010;11:529–535.
41. Bobanovic LK, Royle SJ, Murrell-Lagnado RD. P2X receptor trafficking in neurons is subunit specific. J Neurosci 2002;22:4814–4824.